Diffusion in Fluid Catalytic Cracking Catalysts on Various Displacement Scales and Its Role in Catalytic Performance

P. Kortunov,[†] S. Vasenkov,*[,†] J. Kärger,[†] M. Fé Elía,[‡] M. Perez,[‡] M. Stöcker,[§] G. K. Papadopoulos,[||] D. Theodorou,[||] B. Drescher,[⊥] G. McElhiney,[⊥] B. Bernauer,[#] V. Krystl,[#] M. Kočiřík,[$] A. Zikánová,[$] H. Jirglová,[$] C. Berger,[@] R. Gläser,[@] J. Weitkamp,[@] and E. W. Hansen[+]

Fakultät für Physik und Geowissenschaften, Universität Leipzig, Linnéstrasse 5, D-04103 Leipzig, Germany, Cepsa Research Center, Picos de Europa, 7 Poligono Industrial San Fernando de Henares II, 28850 San Fernando de Henares, Spain, Department of Hydrocarbon Process Chemistry, SINTEF Materials and Chemistry, P.O. Box 124 Blindern Forskningsveien 1, N-0314 Oslo, Norway, School of Chemical Engineering, National Technical University of Athens, 9 Heroon Polytechniou, Zografou Campus, Athens, GR-157 80, Greece, Grace GmbH & Co. KG, In Der Hollerhecke 1, D-67545 Worms, Germany, Institute of Chemical Technology, Technická 5, 166 28 Prague 6, Czech Republic, J. Heyrovský Institute of Physical Chemistry, Dolejškova 3, 182 23 Prague 8, Czech Republic, Institute of Chemical Technology, University of Stuttgart, D-70550 Stuttgart, Germany, and Department of Chemistry, University of Oslo, P.O. Box 1033 Blindern, N-0315 Oslo, Norway

Received January 6, 2005. Revised Manuscript Received February 15, 2005

Diffusivities of *n*-octane in particles of industrial fluid catalytic cracking (FCC) catalysts and in zeolite USY, which is the main zeolitic component of the particles, are reported. Diffusion measurements have been performed by using pulsed field gradient (PFG) NMR for a broad range of molecular displacements and temperatures. The recorded diffusivities are used to evaluate the relevance of various transport modes in the particles of FCC catalysts, such as diffusion in the micropores of the zeolite crystals located in the particles, diffusion through the surface layer of these crystals, and diffusion in the meso- and macropores of the particles, for the rate of molecular exchange between catalyst particles and the surrounding atmosphere. This rate is shown to be primarily related to the diffusion in the meso- and macropores of the particles under the condition of fast molecular exchange between these pores and the zeolite crystals located in the particles. The diffusivity associated with this type of diffusion (i.e., the intraparticle diffusivity) is found to correlate well with the catalytic performance of FCC catalysts having the same fractions of the same zeolite USY but different systems of meso- and macropores.

1. Introduction

The fluid catalytic cracking (FCC) process has been known for around 60 years. It plays a key role in the production of fuels and important raw materials from crude oil. Recent fluctuations in the price and quality of crude oil have underscored the importance of further optimization of fluid catalytic cracking. Due to complexity of this process, fundamental understanding of many aspects of this process is still lacking. One of the most challenging issues, which needs further study, is related to the role of diffusion in the FCC process. The existence of transport limitations under conditions of fluid catalytic cracking has been discussed in a number of recent papers.[1−7] Probably the most common experimental approach which has been used to study transport limitations in FCC catalysts is based on monitoring the influence of the mean size of the zeolite crystals located in catalyst particles on catalytic conversion.[2−5] Provided that there are transport limitations related to intracrystalline diffusion, a decrease of the crystal size is expected to lead to an increase of the conversion rate and/or better selectivity due to faster molecular exchange between zeolite crystals and their surroundings. Depending on the experimental conditions and type of the reactant molecules used, both increased and unchanged conversion rates due to decrease of the crystal size have been observed.[2−5] In addition to this approach, modeling methods and the analytical treatment of experimental data based on the model introduced by Thiele[8]

* To whom correspondence should be addressed. Phone: +49 341 97 32509. Fax: +49 341 97 32549. E-mail: vasenkov@physik.uni-leipzig.de.
[†] Universität Leipzig.
[‡] Cepsa Research Center.
[§] SINTEF Materials and Chemistry.
[||] National Technical University of Athens.
[⊥] Grace GmbH & Co.
[#] Institute of Chemical Technology.
[$] J. Heyrovský Institute of Physical Chemistry.
[@] University of Stuttgart.
[+] University of Oslo.

(1) Bidabehere, C. M.; Sedran, U. *Ind. Eng. Chem. Res.* **2001**, *40*, 530.
(2) Al-Khattaf, S.; de Lasa, H. Catalytic Cracking of Alkylbenzenes. Y-zeolites with Different Crystal Sizes. In *Fluid Catalytic Cracking V. Materials and Technological Innovations*; Ocelli, M. L., O'Connor, P., Eds.; Elsevier: Amsterdam, 2001; Vol. 134, pp 279−292.
(3) Al-Khattaf, S.; Atias, J. A.; Jarosch, K.; de Lasa, H. *Chem. Eng. Sci.* **2002**, *57*, 4909.
(4) Atias, J. A.; Tonetto, G.; de Lasa, H. *Ind. Eng. Chem. Res.* **2003**, *42*, 4162.
(5) Atias, J. A.; de Lasa, H. *Ind. Eng. Chem. Res.* **2004**, *43*, 4709.
(6) Lee, C. K.; Ashtekar, S.; Gladden, L. F.; Barrie, P. J. *Chem. Eng. Sci.* **2004**, *59*, 1131.
(7) Barrie, P. J.; Lee, C. K.; Gladden, L. F. *Chem. Eng. Sci.* **2004**, *59*, 1139.
(8) Thiele, E. W. *Ing. Eng. Chem.* **1939**, *31*, 916.

10.1021/cm050031z CCC: $30.25
Published on Web 03/25/2005

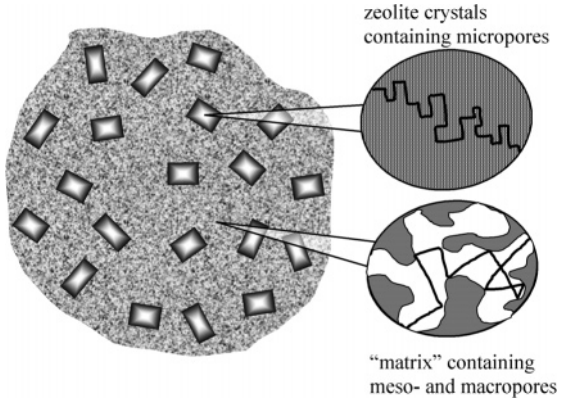

Figure 1. Schematic presentation of a particle of a typical FCC catalyst. The winding lines on the right side schematically show trajectories of the guest molecules.

have been applied for an elucidation of the role of molecular transport in the catalytic performance of FCC catalysts.[1−7] Despite all these efforts a detailed fundamental understanding of transport limitations in the FCC process has not been achieved. This situation is for the most part related to the lack of the direct information on diffusivities in FCC catalysts on various length scales.

Typically, FCC catalysts consist of particles with sizes between 30 and 100 micrometers. These particles contain zeolite crystals in the so-called "matrix".[9] Along with the micropore system of zeolite crystals, the particles also possess a complex system of meso- and macropores located in the matrix (Figure 1). The existence of different types of pore systems in particles of FCC catalysts is expected to result in different modes of diffusion, such as diffusion under molecular confinement in the micropores of the zeolite crystals (i.e., intracrystalline diffusion) and diffusion in the meso- and macropores.

The diffusivity associated with the former mode can be expected to have a much smaller value than that in the meso- and macropores because in the zeolite the molecules constantly remain in close contact with the walls of the micropores. This consideration has often been used to validate the assumption that transport limitations in FCC catalysts are related to intracrystalline diffusion.

In this paper we report the results of the direct measurement of self-diffusion coefficients of guest molecules in FCC catalysts and in USY zeolite by using the pulsed field gradient (PFG) NMR technique.[10−13] This technique has been previously applied for diffusion measurements in various zeolite systems, such as zeolite beds, under conditions when molecular displacements were much smaller than, comparable with, or much larger than the size of individual zeolite particles or crystallites.[11,14] In the present work we extend these studies to industrial FCC catalysts. Using PFG NMR, diffusivities of guest molecules have been measured at different temperatures and for the whole range of the root-mean-square displacements, which is essential for a detailed understanding of molecular transport in FCC catalysts. As a result of this study, the diffusion mechanisms for various displacement scales have been elucidated. The knowledge of the diffusion mechanisms and of the related diffusivities has proved to be essential for an understanding of the role of various mechanisms of diffusion in transport limitations arising during catalytic reactions under typical FCC conditions. Most surprisingly, our data indicate that intracrystalline diffusion does not play a dominant role in transport limitations arising during the FCC process. Instead, these limitations are related to diffusion on the length scale, which is much larger than the size of individual zeolite crystals but at the same time smaller than the size of catalyst particles. To clarify the role of transport limitations in the FCC process the diffusion studies have been complemented by catalytic tests and by the characterization of structural properties of the catalysts used.

Table 1. Results from Nitrogen Adsorption on the As-Synthesized Sample of Large (around 3 μm) NaY Zeolite Crystals and on the Deactivated Sample of USY Zeolite Prepared from the Former Sample

sample	total specific surface area (m^2/g)	specific surface area of micropores (m^2/g)	specific surface area of meso- and macropores (m^2/g)
NaY	831	797	34
deactivated USY	621	504	117

2. Materials and Methods

Sample of Deactivated USY Zeolite with Large Crystal Size. For PFG NMR diffusion measurements of intracrystalline diffusivities a sample of deactivated USY zeolite with a mean crystal size of around 3 μm has been used. The sample was prepared by ammonium-ion exchange and subsequent steaming of a zeolite NaY (Si/Al = 3.4).[15] The steaming was carried out by using the two-step procedure: (i) steaming under the pressure of water vapor of 1 bar at 873 K for 5 h to produce zeolite USY, which was followed by (ii) steaming under the pressure of water vapor of 1 bar at 1088 K for 5 h. The step (ii) is a standard deactivation protocol used by Grace GmbH, Germany. It is applied to simulate zeolite aging, which takes place in a typical FCC unit due to catalyst circulation between the riser reactor and the regenerator. This deactivation protocol has been shown to lead to typical surface areas of meso- and macropores observed in catalysts after aging in FCC units. The results of the standard characterization of the as-synthesized and of the deactivated samples are presented in Table 1. These results show that, as expected, steaming leads to an increase of the surface area of the meso- and macropores and to a decrease of the microporous surface area.

Samples of FCC Catalysts. FCC catalysts were prepared by Grace GmbH, Germany. The catalyst particles (mean size is around 70 μm) were fabricated from a suspension of the industrial USY zeolite, binder, and clay by using spray drying and calcining. All four catalysts studied in the present work contain the same fractions

(9) *Fluid Catalytic Cracking V. Materials and Technological Innovations*; Ocelli, M. L.; O'Connor, P., Eds.; Elsevier: Amsterdam, 2001.
(10) Callaghan, P. T. *Principles of NMR Microscopy*; Clarendon Press: Oxford, 1991.
(11) Kärger, J.; Ruthven, D. M. *Diffusion in Zeolites and Other Microporous Solids*; Wiley & Sons: New York, 1992.
(12) Kimmich, R. *NMR Tomography, Diffusometry, Relaxometry*; Springer: Berlin, 1997.
(13) Blümich, B. *NMR Imaging of Materials*; Clarendon Press: Oxford, 2000.
(14) Kärger, J.; Vasenkov, S.; Auerbach, S. Diffusion in Zeolites. In *Handbook of Zeolite Science and Technology*; Auerbach, S. M., Carrado, K. A., Dutta, P. K., Eds.; Marcel-Dekker Inc.: New York, 2003; pp 341−423.
(15) Berger, C.; Gläser, R.; Rakoczy, R. A.; Weitkamp, J., submitted to *Microporous Mesoporous Mater.*

of the same industrial USY zeolite. The mean size of the zeolite crystals, which consist of many intergrown crystallites, was smaller than 1 μm, i.e., significantly smaller than the mean crystal size of the sample used for PFG NMR measurements of intracrystalline diffusion (see above). Different fabrication conditions have been used for different catalysts in order to prepare samples with different systems of meso- and macropores located in the "matrix" (viz. the nonzeolitic part of the catalyst particles made of binder and clay). All catalysts have been deactivated prior to the measurements by applying a standard deactivation protocol used by Grace. This protocol includes the steaming procedure (ii) described above and the catalyst deactivation by poisoning metals. The deactivation procedure has been designed to model the influence of the catalyst exposure to the typical conditions in an FCC unit.

PFG NMR Measurements. PFG NMR is based on the dependence of the Larmor frequency, which can be understood as the frequency of the rotation of spins around the direction of the applied magnetic field, on the amplitude of the applied field.[10−13] Superimposing a large constant magnetic field by an inhomogeneous field (i.e., so-called magnetic field gradient pulses), the positions of the spins can be labeled by the Larmor frequency and hence also by the phases accumulated due to the rotation with the Larmor frequency. Such labeling is used to monitor molecular diffusivities.

The samples for the PFG NMR measurements were prepared as follows. Around 300 mg of the zeolite or catalyst was introduced into the NMR tube. Then the tube was connected to the vacuum system and the sample was dehydrated by keeping it under high vacuum (less than 10^{-2} mbar) at 673 K for around 40 h. In most cases *n*-octane was used as a probe molecule for diffusion measurements. *n*-Octane was chosen based on the results of the preliminary PFG NMR diffusion studies performed with a number of adsorbates including, in addition to *n*-octane, isobutane, cyclohexane, and neopentane. These studies have revealed that the optimal measurement conditions, especially with respect to the intracrystalline diffusion measurements requiring that the measured root-mean-square displacements are much smaller than the size of zeolite crystals, are achieved with *n*-octane. For measurements of the temperature dependencies of the diffusion coefficients of *n*-octane, the sample has been loaded with this adsorbate from the gas phase by freezing a certain amount of *n*-octane from the calibrated volume of the vacuum system. Upon loading, the NMR tube has been sealed and separated from the vacuum system. For measurements of the diffusion coefficient of *n*-octane at room temperature and for various vapor pressures of *n*-octane, the NMR tube remained connected with the vacuum system during the measurements. This allowed us to change the partial pressure of *n*-octane in the sample without removing the NMR tube from the spectrometer.[16] For measurements of the tortuosity factors for diffusion in the meso- and macropores of catalyst particles by using PFG NMR, 1,3,5-tri-isopropylbenzene was used as an adsorbate. This adsorbate has been chosen because of the large size of the molecules, which excludes their penetration into the micropores of the zeolite. The loading of PFG NMR samples was carried out in this case by introducing a certain amount of the liquid 1,3,5-tri-isopropylbenzene into the PFG NMR tube at room temperature, which was followed by sealing of the tube. Prior to the loading the sample was dehydrated by using the procedure described above.

The diffusivities of *n*-octane in the samples of the deactivated USY zeolite with large crystal size and in the samples of deactivated catalysts have been recorded by using the home-built PFG NMR spectrometer FEGRIS 400 operating at a ^{1}H resonance frequency of 400 MHz.[17] The 13-interval bipolar PFG NMR pulse sequence[18] has been used for the measurement of the diffusion coefficients. This sequence allows suppressing distortions of the PFG NMR results by internal magnetic field inhomogeneities (i.e., internal magnetic field gradients) induced by susceptibility variations in heterogeneous samples. To obtain the diffusivity, an attenuation of the PFG NMR spin−echo signal (Ψ) was measured as a function of the amplitude of the applied field gradient (g). The maximum amplitude of the pulsed field gradients was 35 T/m.

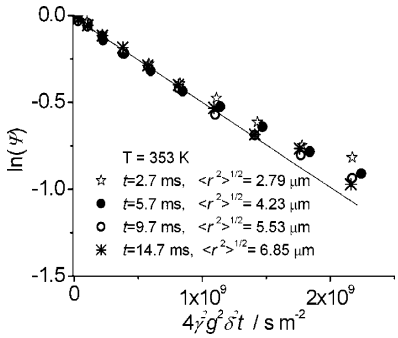

Figure 2. ^{1}H PFG NMR spin−echo attenuation curves measured by using the 13-interval PFG NMR sequence for *n*-octane in a deactivated FCC catalyst. The loading of *n*-octane was 0.6 mmol per 1 g of the zeolite USY in the catalyst. The range of the signal attenuation has been limited by a relatively low (compared with zeolite beds) signal-to-noise ratio.

Catalytic Tests. Tests of the catalytic performance of FCC catalysts have been carried out in the Cepsa Research Center, Spain, by using a fixed bed reactor with a feedstock from the Huelva Refinery. The catalytic cracking has been performed at the reaction temperature 803 K.

Mercury Porosimetry Measurements. Pore size distributions of the meso- and macropores in FCC catalysts were obtained by using the equation suggested by Washburn[19]

$$r = \frac{-2\gamma \cos\theta}{p} \tag{1}$$

where r is the radius of a cylindrical pore, γ is the surface tension of mercury, p is the pressure which must be exerted on the mercury to force it into the cylindrical pore of radius r, and θ is the contact angle. In our measurements we used the value of θ equal to 130°. The measurements were carried out by using an automatic porosimeter (AutoPore III, Micromeritics). During the measurement the pressure in the porosimeter gradually increased from its lowest value, which was equal to 0.01 MPa, up to 400 MPa.

3. Results and Discussion

Determination of the Transport Process Controlling the Rate of Molecular Exchange between the Particles of Industrial FCC Catalyst and Their Surroundings. PFG NMR has been applied to measure *n*-octane diffusivities in samples of FCC catalysts for the root-mean-square displacements $(\langle r^2(t)\rangle)^{1/2}$, which are larger than the size of the zeolite crystals in the particles ($\sim$1 μm) but, at the same time, much smaller than the particle size ($\sim$70 μm). The root-mean-square displacements for diffusion times t and diffusivities D were calculated by applying the Einstein relation $\langle r^2(t)\rangle = 6Dt$. Figure 2 shows examples of the attenuation of the

(16) Valiullin, R.; Kortunov, P.; Kärger, J.; Timoshenko, V. *J. Chem. Phys.* **2004**, *120*, 11804.

(17) Galvosas, P.; Stallmach, F.; Seiffert, G.; Kärger, J.; Kaess, U.; Majer, G. *J. Magn. Reson.* **2001**, *151*, 260.

(18) Cotts, R. M.; Hoch, M. J. R.; Sun, T.; Markert, J. T. *J. Magn. Reson.* **1989**, *83*, 252.

(19) Washburn, E. W. *Proc. Nat. Acad. Sci.* **1921**, *7*, 115.

NMR signal (the "spin−echo") of *n*-octane, which have been recorded under such conditions by using the 13-interval PFG NMR sequence with different diffusion times. Assuming that the diffusion process may be described by the laws of normal (i.e., Fickian) diffusion the attenuation curves obtained with the 13-interval sequence may be presented as[18]

$$\Psi = \exp(-4\gamma^2\delta^2 g^2 D t) \qquad (2)$$

where δ is the duration of the applied gradient pulses with the amplitude g, and γ denotes the gyromagnetic ratio.

Figure 2 shows that the measured attenuation curves exhibit some small systematic deviations from the single-exponential behavior predicted by eq 2. These deviations are most likely related to the existence of an insignificant distribution of the *n*-octane diffusivities over the sample of the FCC catalyst (∼300 mg). It is seen in Figure 2 that the initial slope of the attenuation curves, which represents the effective (i.e., mean) diffusivity, as well the overall shape of the attenuation curves remain essentially unchanged in a broad range of the diffusion times and the corresponding root-mean-square displacements. Combining this observation with the fact that the measurements were performed for displacements much larger than the size of the zeolite crystals located in the particles, it is possible to draw certain conclusions on the rate of molecular exchange between the zeolite crystals and the surrounding meso- and macropores. Slow or incomplete exchange during any particular diffusion time in Figure 2 would results in an observation of fast initial decay of Ψ (i.e., large D) followed by a slower decay.[11] The fast initial decay occurs due to the existence of "fast" *n*-octane molecules, which spend much larger fraction of the diffusion time in the meso- and macropores than the other, i.e., "slow" molecules. The latter molecules are responsible for a slower decay of Ψ mentioned above. The difference between the "fast" and "slow" molecules is expected to become smaller with increasing diffusion time leading to smaller deviations of the measured attenuation curves from the single-exponential behavior predicted by eq 2.

The results in Figure 2 fail to show any significant changes of the attenuation curves with the increasing diffusion time. Hence, we conclude that under the measurement conditions used there was an essentially fast exchange of *n*-octane molecules between the zeolite crystals and the surrounding meso- and macropores.

Plotting the PFG NMR data for the diffusion of *n*-octane in the presentation of Figure 2 for all the temperatures used (i.e., between 253 and 363 K) and for the root-mean-square displacements larger than ∼3 μm but much smaller than the size of the particles (∼70 μm) we have observed qualitatively the same behavior as that shown in Figure 2. This behavior indicates no or only very weak dependence on the diffusion time. It suggests that under the conditions of all these measurements there is fast molecular exchange between the zeolite crystals and the surrounding meso- and macropores. The diffusivities measured under such conditions from the initial slopes of the attenuation curves will be referred to as intraparticle diffusivities.

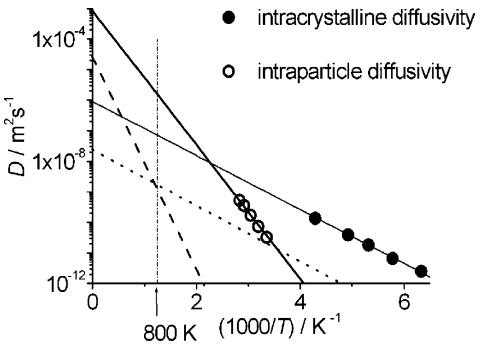

Figure 3. Temperature dependence of the intraparticle diffusivity of *n*-octane in an FCC catalyst and the intracrystalline diffusivity of *n*-octane in the large crystals of USY zeolite measured by PFG NMR. The concentration of *n*-octane in the samples was in all cases 0.6 mmol per 1 g of the zeolite USY. Lines show the results of the extrapolation of the intracrystalline diffusivity (full line) and of the intraparticle diffusivity (fat full line) of *n*-octane to higher temperatures. Also shown in the figure are examples of the temperature dependence of the intracrystalline (dotted line) and the intraparticle diffusivity (dashed line) for alkanes with molecules larger than *n*-octane. The temperature of 800 K is indicated by the dashed−dotted line.

The diffusivities of *n*-octane in the USY crystals located in the particles could not be reliably measured due to the small crystal size. Even at the lowest temperatures and shortest diffusion times accessible for PFG NMR measurements the measured root-mean-square displacements were close to the size of the zeolite crystals. Under these conditions the measured diffusivities may be expected to differ from the true intracrystalline diffusivities due to restrictions of molecular trajectories imposed by the crystal surface.[11,14] Therefore, PFG NMR measurements of the intracrystalline diffusivities of *n*-octane have been performed with the large (∼3 μm) crystals of the deactivated USY zeolite, which has been prepared for the purpose of these measurements. In this case the attenuation curves were found to comply with eq 2 and the measured root-mean-square displacements were much smaller than the crystal size.

Figure 3 shows the temperature dependencies of the intraparticle and intracrystalline diffusivities of *n*-octane, which have been measured for root-mean-square displacements around 3 and 0.5 μm, respectively. These dependencies provide information on the apparent activation energy of diffusion (E_0), which is defined by the Arrhenius law

$$D = D_0 \exp\left(-\frac{E_0}{RT}\right) \qquad (3)$$

where D_0 is a preexponential factor.

It is shown in Figure 3 that the apparent activation energy of intraparticle diffusion is much larger than that of intracrystalline diffusion. Moreover, the value of the former activation energy (43.4 ± 1.3 kJ/mol) turns out to be in satisfactory agreement with the isosteric heat of adsorption of *n*-octane in the catalyst (around 40 kJ/mol for the *n*-octane loading of around 0.6 mmol per 1 g of the zeolite in the catalyst), which has been obtained by measuring the adsorption isotherms of *n*-octane. This suggests that, in complete analogy with the well-known behavior of long-range diffusion in zeolite beds in the Knudsen regime,[11,20−22] the temperature dependence of the intraparticle diffusivity is determined by that of the fraction of adsorbate molecules in

the meso- and macropores of the particles. This analogy is further supported by the following considerations. First, the regime of Knudsen diffusion (characterized by the fact that collisions between molecules are less frequent than those between molecules and the pore walls) can be expected in meso- and macropores of a typical FCC catalyst under typical operating conditions of an FCC unit,[9] as well as under our experimental conditions. Second, under conditions of the measurements of intraparticle diffusivities there is a rapid exchange of *n*-octane between the zeolite crystals and their surroundings. All the considerations discussed above suggest that the intraparticle diffusivity may be presented in the same way as the long-range diffusivity in zeolite beds[11,20−22]

$$D_{\text{intraparticle}} \approx p_{\text{inter}} D_{\text{inter}} = p_{\text{inter}} \frac{1}{\eta_K} \frac{1}{3} \bar{u}\lambda \qquad (4)$$

where p_{inter} and D_{inter} are, respectively, the fraction and the diffusivity of adsorbate molecules in meso- and macropores, and η_K, λ, and $\bar{u}$ are, respectively, the tortuosity factor in the Knudsen regime, the mean free path in the Knudsen regime (which is determined by the mean size of the meso- and macropores), and the mean thermal speed.

The diffusivities presented in Figure 3 have been measured at temperatures which are much lower than those typically used in FCC units (>700 K). This has been done for two reasons: (i) the diffusion measurements at high temperatures would be complicated by the fact that chemical reactions may occur in parallel to diffusion; (ii) the experimental equipment used does not allow measurements at temperatures above 473 K. Although the diffusivities at typical FCC temperatures were not directly recorded, they can be estimated by extrapolating the measured diffusivities to higher temperatures using the Arrhenius law (eq 3) with the same activation energies as those determined at low temperatures. Such an extrapolation can be justified by the following considerations: (i) intracrystalline diffusivities in zeolites can usually be well-described by the Arrhenius law with the activation energy, which is independent of temperature, in an extremely broad temperature range,[11] (ii) for sufficiently long-chain alkanes the activation energy of intracrystalline diffusion is expected to be rather insensitive to the molecular size,[11] and (iii) the apparent activation energy of intraparticle diffusion is primarily determined by the temperature-independent isosteric heat of adsorption in zeolite crystals.

An example of the extrapolation of the measured diffusivities is presented in Figure 3. From the Arrhenius plot in Figure 3 the values of the intraparticle and intracrystalline diffusivities at $T = 800$ K were estimated to be $(2 \pm 0.8) \times 10^{-6}$ m^2/s and $(0.8 \pm 0.2) \times 10^{-7}$ m^2/s, respectively. By relating these diffusivities to the mean size of the regions to which they refer (i.e., the catalyst particle or the zeolite crystal) it is possible to compare the relative importance of intracrystalline and intraparticle diffusion for the rate of molecular exchange between the particles and their surroundings. The comparison can be made by estimating the mean times, τ, which adsorbate molecules spend in the zeolite crystals and in the catalyst particles before leaving them due to the corresponding (viz. intracrystalline or intraparticle) diffusion process. For spherical crystals (particles) the value of τ, which is often referred to as the mean residence time, can be estimated as [11,14,23,24]

$$\tau = \frac{R^2}{15D} \qquad (5)$$

where R is the mean diameter of the crystal (particle) and D is the intracrystalline (intraparticle) diffusivity. Using, respectively, the values of 70 and 1 μm for the mean diameters of the catalyst particles and of the zeolite crystals in the particles we have obtained $\tau = (1.6 \pm 0.6) \times 10^{-4}$ s for the particles and $\tau = (0.8 \pm 0.2) \times 10^{-6}$ s for the zeolite crystals. This estimate shows that the mean residence time in the catalyst particles is around 200 times larger than the corresponding residence time in the zeolite crystals. Hence, we can conclude that the intracrystalline diffusion cannot be expected to determine the rate of the exchange of *n*-octane molecules between the catalyst particles and their surroundings.

It is important to note that this conclusion alone is not sufficient to rule out the possibility that the rate of the *n*-octane exchange between the zeolite crystals and their surroundings determines the corresponding exchange rate between the particles and the surrounding atmosphere because, in general, the former rate depends not only on the intracrystalline diffusivity but also on the permeativity of the zeolite crystal surface. In the limiting case of the permeativity-controlled molecular exchange the expression for the intracrystalline mean residence time (eq 5) has to be replaced by[11,14,23,25]

$$\tau = \frac{R}{3k} \qquad (6)$$

where k is the permeativity of the surface layer of spherical zeolite crystals with the diameter R. In this limiting case, as well as under conditions when both intracrystalline diffusion and surface permeation play a role in the exchange process, our previous estimate of the value of τ based solely on the intracrystalline diffusivity is not valid. Hence, it is necessary to find some other way to make an estimate of the mean residence time in the zeolite crystals. The upper limit of this time in the general case when the intracrystalline diffusion and/or surface permeation control the exchange can be estimated by using the results of the measurements of intraparticle diffusivities. These results show that there is fast exchange of *n*-octane between the zeolite crystals and their surroundings for displacements around 3 μm or larger. In particular, fast exchange has been observed at 353 K for the diffusion time 2.7×10^{-3} s. (Figure 2). Hence, the mean residence time in the zeolite crystals is expected to be several

(20) Kärger, J.; Kočiřik, M.; Zikanova, A. *J. Colloid Interface Sci.* **1981**, *84*, 240.
(21) Geier, O.; Vasenkov, S.; Kärger, J. *J. Chem. Phys.* **2002**, *117*, 1935.
(22) Vasenkov, S.; Geier, O.; Kärger, J. *Eur. Phys. J. E* **2003**, *12* (1), 35.
(23) Barrer, R. M. *Zeolites and Clay Minerals as Sorbents and Molecular Sieves*; Academic Press: London, 1978.
(24) Kočiřik, M.; Zikánová, A. *Z. phys. Chemie, Leipzig* **1972**, *250*, 250.
(25) Kočiřik, M.; Struve, P.; Fiedler, K.; Bülow, M. *J. Chem. Soc., Faraday Trans. 1* **1988**, *84*, 3001.

times smaller than the diffusion time, i.e., around 10^{-3} s or smaller. For the two limiting cases of the *n*-octane exchange controlled by the intracrystalline diffusion and by the permeation of the surface layer of zeolite crystals we can extrapolate this value to $T = 800$ K by using eqs 5 and 6. These equations show that the temperature dependence of $1/\tau$ may be described in the same way as those of D and k, i.e., by the Arrhenius law of the type of eq 3. Noting that the activation energy of the surface permeativity can be expected to be larger than that of intracrystalline diffusivity; the upper limit of the intracrystalline mean residence time at 800 K is estimated to be $(4 \pm 1) \times 10^{-5}$ s by using the latter activation energy (16.9 ± 0.1) kJ/mol. The real value of the mean residence time, especially in the case of the molecular exchange limited by the permeation of the surface layer with the activation energy larger than that of the activation energy of intracrystalline diffusion, is expected to be much smaller than this limiting value. Hence, it is also much smaller than our estimate of the intraparticle mean residence time $((1.6 \pm 0.6) \times 10^{-4}$ s), which is based on the intraparticle diffusivity. This comparison shows that the intraparticle diffusion is the most relevant diffusion mode for the exchange of *n*-octane molecules between the catalyst particles and the surrounding atmosphere.

We have extended our extrapolation to alkanes larger than *n*-octane. It is reasonable to assume that the preexponential factors of both intraparticle and intracrystalline diffusivities will decrease with increasing size of the guest molecules. In the Knudsen regime the activation energy of intraparticle diffusion is determined by the isosteric heat of adsorption and thus increases with increasing molecular size. The resulting temperature dependence of the intraparticle diffusivity is shown in Figure 3 as a dashed line. In contrast to intraparticle diffusion, for sufficiently long-chain alkanes the activation energy of the intracrystalline diffusivities can be expected to be essentially independent of molecular size.[11] Hence, in the presentation of Figure 3 the temperature dependence of the intracrystalline diffusivity of the larger alkanes (dotted line) is simply shifted parallel to that of *n*-octane. Thus Figure 3 demonstrates that the difference between the intracrystalline and intraparticle diffusivities at around 800 K decreases with increasing size of the molecules. The activation energy of the permeativity of the zeolite crystal surface may increase with the increasing size of adsorbate molecules. However, it is unlikely that this increase will be of the same order of magnitude or larger than the increase in the activation energy of the intraparticle diffusivity, which is determined by the isosteric heat of adsorption. As a result, a decrease in the value of the intraparticle diffusivity at typical FCC temperatures with increasing size of adsorbate molecules is expected to be larger than or of the same order of magnitude as the corresponding changes in the intracrystalline diffusivity and in the permeativity of the zeolite crystal surface. On the basis of this estimate we may conclude that for the alkanes of the same size as *n*-octane, as well as for larger molecules, the rate of molecular exchange between the catalyst particles and their surroundings is primarily determined by intraparticle diffusion. The important consequence of this conclusion

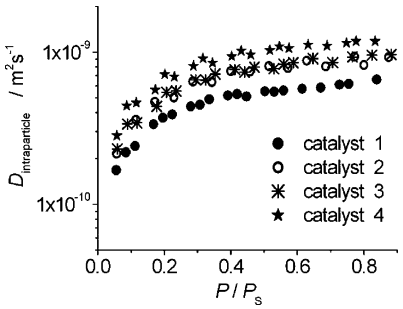

Figure 4. Dependence of intraparticle diffusivities of *n*-octane in the catalyst samples on the relative pressure of *n*-octane in the gas phase. The measurements have been performed at 297 K under equilibrium with the adsorbed phase. P_s denotes the saturated vapor pressure of *n*-octane at 297 K.

is that for a prevailing fraction of species both in feed and product of cracking process the transport limitation during FCC catalytic reactions is not at all related to the intracrystalline diffusion or the permeation of the surface layer of the zeolite crystals. Instead, the transport mechanism of relevance is that of intraparticle diffusion.

It is interesting to note that recent results of uptake studies of several hydrocarbons (including *n*-octane) in FCC catalysts at temperatures close to those used in the present study suggest that the rates of adsorption/desorption of these hydrocarbons are controlled by the permeation of the surface layer of the zeolite crystals located in the catalyst particles.[6,7] An important difference between these studies and the PFG NMR studies reported in the present paper is related to the fact that the PFG NMR diffusion measurements are performed under equilibrium conditions characterized by the absence of concentration and temperature gradients. Direct PFG NMR observation of fast exchange of *n*-octane molecules between the zeolite crystals located in the particles and the surrounding meso- and macropores at temperatures as high as 353 K shows that under our measurement conditions the permeation of the surface of the zeolite crystals does not play an essential role in the overall transport through the particles.

Correlating Molecular Transport with Catalytic Performance. To confirm our conclusion about the relevance of intraparticle diffusion for transport limitations during FCC catalysis a set of four samples of deactivated FCC catalysts with the same fraction of the same zeolite USY, but with different properties of the meso- and macropore system in the matrix, has been prepared. The intraparticle diffusivities of *n*-octane have been measured for different pressures of *n*-octane in the sample at a fixed temperature of 297 K (Figure 4) and for different temperatures between 253 and 363 K for a fixed *n*-octane loading of 0.6 mmol/g (Figure 5).

Figures 4 and 5 show that for all the temperatures and concentrations used the relation between the intraparticle diffusivities of *n*-octane in different catalysts remain essentially the same. Catalyst 4 exhibits the largest intraparticle diffusivities. Catalysts 3 and 2 show lower diffusivities, while those in the reference Catalyst 1 sample have the smallest values. There is a good correlation between the intraparticle diffusivities and the catalytic performance as assessed by

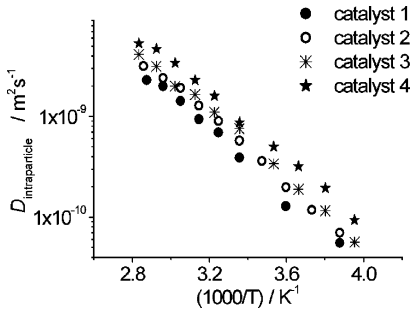

Figure 5. Temperature dependence of intraparticle diffusivities of *n*-octane in the samples of FCC catalysts. The loading of *n*-octane was in all cases 0.6 mmol/g.

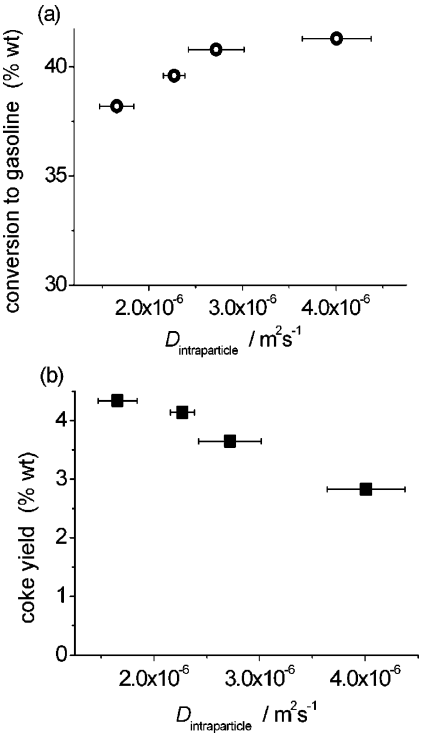

Figure 6. Correlation between the intraparticle diffusivities of *n*-octane extrapolated to 803 K for the loading of *n*-octane in the catalyst of 0.6 mmol/g and catalytic performance expressed by the oil-to-gasoline conversion for the same catalyst-to-oil ratios equal to 4.0 (a), and by the coke yield for the same conversion of oil equal to 52 wt % (b). The reaction temperature was 803 K.

the standard micro activity test (MAT). In particular, the total conversion of oil and the conversion of oil to gasoline for the same catalyst-to-oil ratios have been found to increase and the coke yield for the same conversion has been found to decrease with increasing intraparticle diffusivity. Figure 6 shows examples of the observed correlations.

One of the important features of intraparticle diffusion is related to the fact that the activation energy of this process is expected to coincide with the isosteric heat of adsorption. Hence, such a coincidence can be used as a "fingerprint" of intraparticle diffusion. Recent results reported in the literature revealed that at least under certain reaction conditions the diffusion process responsible for transport limitations during FCC catalysis exhibits this "fingerprint". In particular, application of the model based on the Thiele concept to the results of the tests of commercial FCC catalysts by using a Riser Simulator reactor has shown that there is good

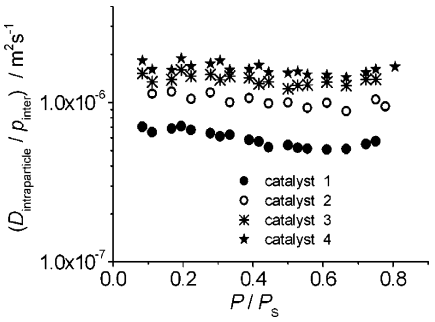

Figure 7. $D_{intraparticle}/p_{inter}$ as a function of the relative pressure of *n*-octane for different catalysts at 297 K.

agreement between the activation energy of the diffusion process responsible for transport limitations and the heat of adsorption.[1] Our results reported above suggest that this agreement is not at all coincidental. It may, in fact, reveal the nature of the diffusion process responsible for transport limitations.

Relationship between Intraparticle Diffusion and the Structure of the FCC Catalyst Particles. Equation 4 can be applied for an elucidation of the role of various structural parameters of catalyst particles in the observed enhancement of the intraparticle diffusivities in the set of catalyst samples discussed above. Using the results of the measurement of the adsorption isotherms of *n*-octane and of N_2, the fraction of *n*-octane molecules in the meso- and macropores (p_{inter} in eq 4) has been determined for all four catalysts. Figure 7 shows the dependence of the values of $D_{intraparticle}/p_{inter}$ on the relative pressure of *n*-octane for different catalysts. It is seen that, within the experimental uncertainty, the values of $D_{intraparticle}/p_{inter}$ for each catalyst do not depend on the relative pressure of *n*-octane. This is in agreement with eq 4 because, with the exception of p_{inter}, all the other parameters in the right part of eq 4 (including λ, which is determined by the mean size of the meso- and macropores) are expected to be independent of the relative pressure of *n*-octane. Figure 7 indicates that the differences between the intraparticle diffusivities do not vanish after dividing $D_{intraparticle}$ by p_{inter}. Hence, p_{inter} cannot be primarily responsible for these differences.

As a second parameter, the tortuosity factor has been evaluated. It has been determined by the PFG NMR diffusion measurements of a liquid adsorbate in the meso- and macropore systems of the particles. Owing to the large size of the molecules, which excludes their penetration into the micropores of the zeolite, 1,3,5- tri-isopropylbenzene has been chosen for this purpose. Using PFG NMR the unrestricted diffusivity of 1,3,5-tri-isopropylbenzene in the liquid phase (2.3×10^{-10} m^2/s) and the corresponding diffusivities in the meso- and macropore systems of the particles at 298 K have been measured. The latter diffusivities have been obtained from the measured PFG NMR attenuation curves by assuming the existence of at least two fractions of 1,3,5-tri-isopropylbenzene molecules during typical times of the diffusion measurements: the molecules diffusing in large pores formed by the gaps between catalyst particles and those diffusing in intraparticle meso- and macropores.[26] The

(26) Vasenkov, S.; Kortunov, P. *Diffus. Fund.* **2005**, in press.

Table 2. Tortuosity Factors for the Diffusion of 1,3,5-Tri-isopropylbenzene in the Meso- and Macropores of the Catalyst Particles

FCC catalyst	η
catalyst 1	1.42
catalyst 2	1.67
catalyst 3	1.89
catalyst 4	1.75

tortuosity factors have been calculated by dividing the unrestricted diffusivity of 1,3,5-tri-isopropylbenzene in the liquid phase by that in the intraparticle pores. The results are presented in Table 2. Comparison of the intraparticle diffusivities in Figure 6 with the data in Table 2 indicates that the observed differences between the tortuosity factors cannot be considered as the main reason for the different intraparticle diffusivities in our set of catalyst samples.

The only parameter left in eq 4 which may explain differences between the intraparticle diffusivities is the mean free path, λ. Hence, on the basis of the above discussion, we may conclude that these differences are primarily related to similar differences in the values of λ, which are determined by the mean size of the intraparticle meso- and macropores.

This conclusion has been confirmed by the results of the mercury porosimetry measurements of the pore size distributions in the catalysts (Figure 8).

The mercury porosimetry measurements have revealed the existence of the following three types of meso- and macropores, which can be clearly seen in the insert of Figure 8: (a) meso- and macropores with sizes smaller than 20 nm, (b) macropores with a mean size around 100 nm, and (c) macropores with a mean size around 10 000 nm. The pores of the type (c) are sufficiently large to be assigned to the space between catalyst particles, while the pores of the types (a) and (b) are, obviously, intraparticle pores. For comparison, Figure 8 also shows the values of λ, which have been calculated by using eq 4 with the experimentally determined values of $D_{\text{intraparticle}}$, p_{inter}, and η and with the values of the mean thermal speed given by

$$\bar{u} = (8RT/\pi M)^{1/2} \tag{7}$$

where R is the gas constant and M is the molar mass. It is seen that the calculated values of λ (straight lines in Figure 8) increase with increasing catalyst numbers in the same way as the maxima of the size distribution for the macropores of type (b) as well as the mean sizes of these macropores (arrows in Figure 8). It can also be seen that the values of λ appear to be systematically smaller than the corresponding mean sizes of the macropores of type (b) (compare the straight lines and arrows in Figure 8). The presence of the macropores and mesopores of type (a) is, clearly, one of the reasons for the existence of this discrepancy. However, it is unlikely to be the main one due to the following two observations: (i) the pores of type (a) account for only around one-third (or less) of the volume of all intraparticle meso- and macropores (i.e., of the pores of types (a) and (b)), and (ii) the discrepancies between the value of λ and the corresponding mean sizes of the pores of type (b) are in the range of or larger than a factor of 2. Assuming the same molecular density in all types of pores the observation (i) suggests that the mean free path in the Knudsen regime for the pores of types (a) and (b) cannot be more than 33% smaller than the corresponding value for the pores of the type (b). In our opinion, the main reason for the systematic differences between the values of λ and the corresponding mean sizes of the macropores of type (b) is related to the fact that the former values have been calculated by using the tortuosity factors for the diffusion of liquid adsorbate rather than for gas diffusion in the Knudsen regime, which is relevant for the present study. The tortuosity factors in random porous systems tend to be higher for the latter type of diffusion than those for the former one.[21,22,27,28] Alternatively, if one wants to keep the same tortuosity factors for both regimes it is necessary to use values of λ, which are significantly smaller than the corresponding mean pore sizes.[29] In our opinion, from the experimental point of view the latter approach does not offer any additional advantages in comparison to the former one because there is no simple experimental way to estimate the "correct" values of λ resulting in the tortuosity factors, which do not depend on the diffusion regime.

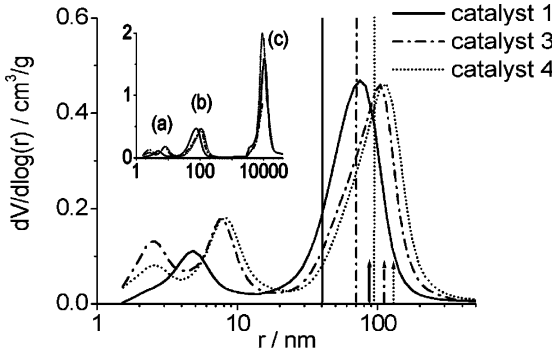

Figure 8. Comparison of the pore size distributions (curves) for intraparticle meso- and macropores obtained by mercury porosimetry with the values of the mean free path for the Knudsen diffusion (vertical lines), which were calculated by using eq 4 with the experimentally determined values of $D_{\text{intraparticle}}$, p_{inter}, and η. Arrows indicate the mean sizes of the macropores of the type (b). The mean sizes have been calculated as first statistical moments for the peaks of the type (b), i.e., by using volume averaging. The insert shows the pore size distributions for all meso- and macropores in the catalyst samples as measured by mercury porosimetry. One can see the following three types of pores: (a) meso- and macropores with sizes smaller than 20 nm, (b) macropores with a mean size around 100 nm, and (c) macropores with a mean size around 10 000 nm.

4. Conclusions

Here we report the results of PFG NMR measurements of the diffusivities of *n*-octane in particles of FCC catalyst and in the crystals of USY zeolite, which represent the most important catalytically active part of the particles. Our results show that for guest molecules which are at least as large as *n*-octane the rate of molecular exchange between catalyst particles and their surroundings is primarily determined by the coefficient of intraparticle diffusion. This diffusion coefficient may be satisfactorily described as a product of the fraction of guest molecules in the meso- and macropores of the particles and their diffusivities. Hence, intraparticle

(27) Burganos, V. N. *J. Chem. Phys.* **1998**, *109*, 6772.
(28) Vignoles, G. L. *J. Phys. IV* **1995**, *5*, 159.
(29) Zalc, J. M.; Reyes, S. C.; Iglesia, E. *Chem. Eng. Sci.* **2004**, *59*, 2947.

diffusivity does not directly depend on the diffusion coefficient in the micropores of the zeolite crystals (i.e., on the intracrystalline diffusivity). In the present work we have directly demonstrated that the intraparticle diffusivity may be increased by increasing the mean size of the macropores in the particles. This opens a possibility to optimize the transport properties of catalysts without changing the zeolitic part of the catalyst particles. The latter part is mostly responsible for chemical transformations and can be considered as being optimized already with respect to these transformations.

Acknowledgment. This work has been done under coordination of Leipzig University, Germany in the framework of the "TROCAT" project (contract G5RD-CT-2001-00520), which is funded by the European Community under the "Competitive and Sustainable Growth" Programme.

CM050031Z